Journal of Molecular Structure 982 (2010) 22–27

Contents lists available at ScienceDirect

Journal of Molecular Structure

journal homepage: www.elsevier.com/locate/molstruc

FT-IR, UV spectroscopic and DFT quantum chemical study on the molecular conformation, vibrational and electronic transitions of 2-aminoterephthalic acid

Mehmet Karabacak [a,*], Mehmet Cinar [a], Zeliha Unal [a], Mustafa Kurt [b]

[a] Department of Physics, Afyon Kocatepe University, 03040 Afyonkarahisar, Turkey
[b] Department of Physics, Ahi Evran University, 40100 Kırşehir, Turkey

ARTICLE INFO

Article history:
Received 17 May 2010
Received in revised form 15 July 2010
Accepted 16 July 2010
Available online 10 August 2010

Keywords:
Infrared and UV spectra
HOMO and LUMO
DFT
2-Aminoterephthalic acid

ABSTRACT

In this work, the molecular conformation, vibrational and electronic analysis of 2-aminoterephthalic acid are presented for the ground state using FT-IR experimental technique and density functional theory (DFT) employing B3LYP exchange correlation functional with the 6-311++G(d,p) basis set. FT-IR spectrum was recorded in the region of 400–4000 cm^{-1}. The ultraviolet absorption spectrum of studied compound that dissolved in ethanol was examined in the range of 190–450 nm. The complete assignments of fundamental vibrations were performed on the basis of the total energy distribution (TED) of the vibrational modes, calculated with scaled quantum mechanics (SQM) method. Optimized structure of title compound was interpreted and compared with the earlier reported experimental values of a similar compound. A study on the electronic properties, such as HOMO and LUMO energies, were performed by time-dependent DFT (TD-DFT) approach.

1. Introduction

Terephthalic acid (TPA) is useful in making condensation polymers and its preparation by autoxidation of *p*-xylene has received much attention [1]. TPA is primarily used in the manufacture and production of polyester fibers, films, polyethylene terephthalate solid-state resins and polyethylene terephthalate engineering resins. As a derivative of TPA, the 2-aminoterephthalic (2-ATA) acid is good organic building block for construction of extended open framework.

The crystal structure of TPA was defined by Bailey and Brown [2]. The FT-IR and Raman spectra, vibrational assignment and ab initio calculations of TPA and related compounds were reported [3]. Three crystal structures of TPA salts of simple amines were determined [4]. Barreto et al. [5] investigated the suitability of TPA as a hydroxyl radical dosimeter for general use in biologically relevant reactions. The FT-IR and Raman spectra, semi empirical AM1 and PM3; MP2/DZV and DFT/B3LYP-6-31G(d) ab initio calculations for dimethylterephthalate (DMT) were investigated [6]. The five new lanthanide coordination polymers with 2-ATA and 1,10-phenanthroline were prepared by hydrothermal reactions and structurally characterized by Liu et al. [7]. The series of lanthanide complexes with 2-ATA under the standard conditions was obtained [8]. Conducting copolymers based on aniline and 2-ATA have been chemically synthesized and characterized by several techniques [9]. Southern et al. presented the electronic spectroscopy of anthranilic acid including fluorescence excitation and dispersed emission spectra in a supersonic jet [10]. The fluorescence-dip infrared spectra of anthranilic acid in both its ground and first-excited electronic states were also presented.

Till now not only a detailed analysis of vibrational frequencies but also conformational and electronic analysis of 2-ATA has not been reported. As a result we set out experimental and theoretical investigation of the conformation, vibrational and electronic transitions of this molecule. The density functional theory (B3LYP) calculations have been performed. The geometric structure, vibrational wavenumbers, HOMO–LUMO energies, absorption wavelengths, excitation energies and electric dipole moment (μ) of 2-ATA have been studied. A detailed interpretation of the vibrational spectra of 2-ATA has been made on the basis of the calculated total energy distribution (TED).

2. Experimental

The 2-aminoterephthalic acid was purchased from Sigma–Aldrich Company with a stated purity 99% and was used as such without further purification. The FT-IR spectrum (4000–400 cm^{-1}) of a KBr disc of the sample was recorded on a Perkin Elmer FT-IR System Spectrum BX spectrometer. The ultraviolet absorption spectrum of 2-ATA was examined in the range 190–450 nm using Shimadzu UV-1700 PC, UV–VIS recording Spectrophotometer. The UV pattern is taken from a 10^{-5} molar solution of 2-ATA, solved in ethanol.

* Corresponding author. Tel.: +90 272 2281311; fax: +90 272 2281235.
E-mail address: karabacak@aku.edu.tr (M. Karabacak).

0022-2860/$ - see front matter © 2010 Elsevier B.V. All rights reserved.
doi:10.1016/j.molstruc.2010.07.033

3. Quantum chemical calculations

The first task for the computational work was to determine the optimized geometry of the present compound. Since the experimental geometries of free 2-ATA is not available, the spatial coordinate positions of 2-aminoterephthalic acid dimethylester, as obtained from an X-ray structural analysis [11], were used as the initial coordinates for the theoretical calculations. The hybrid B3LYP method [12,13] based on Becke's three-parameter functional of DFT and 6-311G++(d,p) basis set level were chosen. In connection with the hydrogen orientations of the oxygen atom of the carboxylic acid groups, 2-ATA may have 16 different possible structures. The calculated energies and energy difference of 16 structures for title molecule are presented in Table S1 and the optimized possible geometric structures are gathered in Fig. S1 (supporting information). Our calculations demonstrate that structure C1 has the lowest energy and the most stable one which shows agreement with crystallographic geometric structure of 2-aminoterephthalic acid dimethylester [11]. Optimized structural parameters were used to calculate the vibrational IR spectrum. The stability of the optimized geometries was confirmed by wavenumber calculations, which gave positive values for all obtained wavenumbers. We know that DFT potentials systematically overestimate the vibrational wavenumbers [14]. These discrepancies are corrected either by computing anharmonic corrections explicitly [15] or by introducing a scaled field or by directly scaling the calculated wavenumbers with a proper factor. Considering systematic errors with a scaling factor of 0.983 up to 1700 cm^{-1} and 0.958 for greater than 1700 cm^{-1} [16,17], we calibrated the vibrational wavenumbers calculated by B3LYP with 6-311++G(d,p) basis set.

TED calculations, which show the relative contributions of the redundant internal coordinates to each normal vibrational mode of the molecule and thus enable us numerically to describe the character of each mode, were carried out by the scaled quantum mechanical (SQM) program [18,19] using the output files created at the end of the wavenumber calculations. Calculations were done for 16 conformers of the compound in the ground state, and tabulated only for the most stable structure (C1). All calculations were performed by using the Gaussian 03 program package on a personal computer [20].

4. Results and discussion

4.1. Molecular geometry

The optimized structure of title compound is shown in Fig. 1 with numbering of the atoms. The optimized structure parameters of studied molecule are listed in Table 1, in accordance with the atom numbering scheme given in Fig. 1. The available experimental data [11] obtained by the X-ray study for a similar compound is also given in Table 1 for comparison. As can be noticed from Table 1, most of the computed bond lengths and bond angles are slightly larger than experimental ones. These discrepancies can be explained by the fact that the calculations assume an isolated molecule where the intermolecular Coulombic interaction with the neighboring molecules are absent, whereas the experimental result corresponds to interacting molecules in the crystal lattice. In the X-ray diffraction experiment, large deviation from experimental C–H and N–H bond lengths may arise from the low scattering factors of hydrogen atoms. On the other hand, it is commonly known that the X-ray diffraction method does not inform properly about such bonds. One should apply the neutron diffraction methods which informs on the position of nuclei and not on the electron density distribution. Therefore, C–H and N–H bond lengths are not discussed in this study.

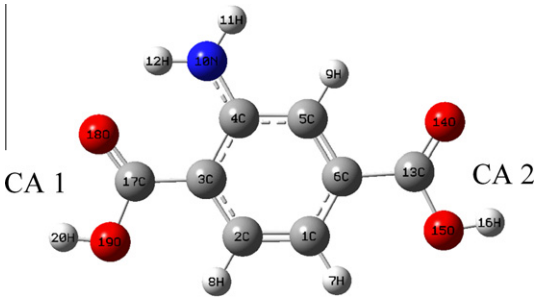

Fig. 1. The theoretical optimized possible geometric structure with atoms numbering of 2-ATA.

Table 1
Comparison of the theoretical and experimental geometric parameters of 2-ATA according to atom numbers given in Fig. 1, bond lengths in angstrom and bond angles in degrees.

Bond lengths (°)	Exp[a]	B3LYP	Bond angles (Å)	Exp.[a]	B3LYP
C1–C2	1.376	1.381	C2–C3–C17	119.9	120.3
C1–C6	1.379	1.407	C4–C3–C17	120.5	120.2
C2–C3	1.403	1.408	C3–C4–C5	117.7	117.8
C3–C4	1.398	1.425	C3–C4–N10	123.9	122.6
C3–C17	1.489	1.470	C5–C4–N10	118.4	119.6
C4–C5	1.418	1.411	C4–C5–C6	121.0	121.4
C4–N10	1.365	1.361	C4–C5–H9	119.5	119.8
C5–C6	1.368	1.385	C6–C5–H9	119.5	118.8
C6–C13	1.512	1.492	C1–C6–C5	121.3	120.8
N10–H11	0.920	1.005	C1–C6–C13	121.7	122.0
N10–H12	0.940	1.010	C5–C6–C13	117.0	117.3
C13–O14	1.195	1.209	C4–N10–H11	111.0	119.7
C13–O15	1.330	1.356	C4–N10–H12	120.0	119.1
O15–H16	–	0.969	H11–N10–H12	122.0	120.2
C17–O18	1.216	1.221	C6–C13–O14	124.3	125.0
C17–O19	1.333	1.357	C6–O13–O15	111.9	112.9
O19–H20	–	0.968	O14–C13–O15	123.8	122.1
$C–H_{average}$	0.950	1.082	C13–O15–H16	–	106.8
r.m.s.		0.045	C3–C17–O18	124.8	125.7
Bond angles (Å)			C3–C17–O19	112.9	113.8
C2–C1–C6	118.7	118.6	O18–C17–O19	122.3	120.5
C2–C1–H7	120.6	121.0	C17–O19–H20	–	106.4
C6–C1–H7	120.6	120.4	r.m.s.		1.9
C1–C2–C3	121.6	121.9	Selected dihedral angles		
C1–C2–H8	119.2	119.9	C3–C4–N10–H11		5.8
C3–C2–H8	119.2	118.2	C3–C4–N10–H12		5.0
C2–C3–C4	119.6	119.5			

[a] Ref. [11].

In the title molecule studied here introduction of two substituent groups on the benzene ring causes some changes in the ring C–C bond distances and also the position of the substituents in the benzene ring as well as its electron donor/acceptor capabilities plays a vital role on the structural and electronic properties of the molecules. Amino substituted benzenes were shown to be non-planar in the ground state both experimentally [21–23] and theoretically [24–26]. The two amino hydrogens were calculated with dihedral angles of 5° and 5.8° which provide a good measure of planarity. For aniline these dihedral angles were calculated at 8° and 12° for antranilic acid [10]. The amino hydrogen closer to the carboxyl group (H12) is more nearly planar than the other amino hydrogen and the N–H12 bond length was computed slightly longer than the N–H11 bond length by 0.005 Å. The optimized bond lengths of C–C in ring are computed in the range from 1.381 to 1.425 Å which is in good agreement with those in crystal structure (1.368–1.418 Å). The C–COOH (1) and C–COOH (2) bond lengths are predicted about 0.02 Å shorter than experimental results. Due

to the Coulombic interaction between O(18) and H(12) this bond length was recorded and calculated larger than the C(13)–O(14) double bond. The similar effect can also be seen for bond angles between ring and carboxylic acid groups. The reminder bond angles show good agreement with recorded values, except the CNH angles. To make comparison with experimental data, we present r.m.s. values based on the calculations (bottom of Table 1). As can be seen there, the average deviation of bond lengths and bond angles is obtained at 0.045 Å and 1.9°, respectively.

4.2. Vibrational analysis

The recorded FT-IR and calculated vibrational wavenumbers along with their relative intensities and probable assignments with

Table 2
The observed FT-IR and calculated wavenumbers (in cm^{-1}) using B3LYP/6-311++G(d,p) along with their relative intensities, probable assignments and total energy distribution (TED) of 2-ATA.

	Experimental	6–311++G(d,p)			Assignments based on TED (≥10%)
	FT-IR	Unscaled	Scaled	I_{IR}	
1		3774	3616	109.86	νOH_{CA1} (100)
2		3770	3611	118.00	νOH_{CA2} (100)
3	3507	3712	3556	75.96	ν_{asym} NH_2 (100)
4	3393	3555	3406	114.31	ν_{sym} NH_2 (100)
5		3226	3090	0.26	νCH (100)
6		3210	3075	0.41	νCH (100)
7	3055	3185	3052	3.52	νCH (100)
	2986				Overtone/combination
	2887				Overtone/combination
	2712				Overtone/combination
	2644				Overtone/combination
	2576				Overtone/combination
	2533				Overtone/combination
8		1787	1712	354.79	$\nu C{=}O_{CA2}$ (83)
9	1686	1743	1670	404.66	$\nu C{=}O_{CA1}$ (71)
10	1625	1660	1632	95.88	νCC_{ring} (54)
11	1591	1626	1598	235.00	ρNH_2 (59) + νCC_{ring} (19)
12	1553	1580	1553	82.84	νCC_{ring} (53) + ρNH_2 (20)
13	1496	1524	1498	35.17	βCH(49) + νCC_{ring} (29)
14	1453	1465	1440	84.76	νCC_{ring} (29) + $\nu C{-}NH_2$ (23)
15	1419	1392	1368	22.99	νCC_{ring} (40) + $\nu C{-}CA_1$ (11)
16		1368	1345	177.85	βOH_{CA2} (18)
17	1316	1355	1332	74.95	νCC_{ring} (24) + βOH_{CA1} (15) + βOH_{CA2} (12)
18		1312	1290	13.47	βCH (63)
19	1233	1306	1283	13.68	νCC_{ring} (28) + $\nu C{-}NH_2$ (25) + βCH (10)
20		1199	1179	259.05	βOH_{CA1} (29) + νCC_{ring} (24) + $\nu C{-}CA_1$ (15) + βCH (14)
21		1186	1166	393.52	βOH_{CA2} (31) + $\nu C{-}CA_2$ (13) + $\nu C{-}OH_{CA1}$ (11)
22		1177	1157	114.02	βCH (43) + νCC_{ring} (14)
23	1121	1128	1109	63.34	βCH (24) + νCC_{ring} (23) + $\nu C{-}OH_{CA2}$ (21) + r NH_2 (10)
24		1089	1070	187.67	$\nu C{-}OH_{CA1}$ (41) + r NH_2 (20) + νCC_{ring} (10)
25		1054	1036	6.61	νCC_{ring} (36) + r NH_2 (30)
26		986	969	0.09	γCH (92)
27	915	957	941	40.57	βCCC_{ring} (29) + νCC_{ring} (14) + $\nu C{-}OH_{CA2}$ (14) + $\nu C{-}NH_2$ (12)
28	880	910	894	11.81	γCH (87)
29	831	850	835	0.04	γCH (57) + γCCC_{ring} (20)
30	782	806	792	0.62	$\gamma CCOO_{CA+CA2}$ (56)
31		768	755	99.11	$\gamma CCOO_{CA1+CA2}$ (46) + γCH (33)
32	753	757	745	5.08	Ring breathing (42)
33	690	728	716	101.81	$\beta OCOH_{CA1}$ (11) + $\beta OCOH_{CA2}$ (10) + $\nu C{-}CA_2$ (10)
34	676	709	697	13.17	γCCC (44) + $\gamma CCOO_{CA1}$ (28)
35		651	640	21.28	ρCA_2 (36) + ρCA_1 (22)
36		618	608	118.62	γOH_{CA2} (45) + γNH of NH_2 (14)
37		609	599	1.84	τNH_2 (69)
38	587	584	574	3.75	βCCC (49)
39		564	554	2.42	rCA_2 (32) + rNH_2 (14) + rCA_1 (13)
40		559	549	57.45	γOH_{CA1} (87)
41		538	529	22.72	γOH_{CA2} (40) + γCCC (28)
42	491	501	492	16.99	$\nu C{-}CA_2$ (15) + $\nu C{-}CA_1$ (13) + $\beta CC{=}O_{CA2}$ (23) + ρCA_1 (14)
43		454	446	11.89	rCA_1 (38) + rCA_2 (22)
44		436	428	23.13	γCCC_{ring} (79)
45		374	368	5.75	rNH_2 (55)
46		303	297	2.17	βCCC (20) + $\nu C{-}CA_2$ (15) + $\nu C{-}CA_1$ (13) + $\beta CC{-}CA_1$ (11)
47		266	261	11.08	rCA_1 (48) + rCA_2 (13)
48		261	257	7.43	γCCC (46) + γCCNH (19)
49		231	227	123.58	τNH_2 (61) + γCCC (21)
50		163	160	43.22	γCCC (50) + τNH_2 (25)
51		158	155	4.34	rCA_1 (60) + rCA_2 (19)
52		78	76	0.13	τCA_1 (68) + $\gamma CCOH_{CA2}$ (11)
53		65	64	6.66	$\gamma CCOH_{CA1}$ (60) + $\gamma C{-}CA_2$ (15)
54		52	51	0.41	τCA_2(81)

ν_{sym} – ν_{asym}; symmetric–asymmetric stretching, β; in-plane bending, γ; out-of-plane bending, ρ; scissoring, r; rocking, τ; torsion (wavenumbers (cm^{-1}), IR intensities; I_{IR} ($K\ mmol^{-1}$)).

TED of title molecule are given in Table 2. The experimental and simulated infrared spectra of 2-ATA are shown in Fig. 2, where the calculated intensity is plotted against the wavenumbers. It should be noted that the calculations were made for a free molecule in vacuum, while experiments were performed for solid samples. Furthermore, the anharmonicity is neglected in the real system for the calculated vibrations. Therefore, there are disagreements between the calculated and observed vibrational wavenumbers.

The aromatic structure shows the presence of C–H and N–H stretching vibrations above 3000 cm^{-1} which is the characteristic region for ready identification of this structure [27,28]. These are usual range of appearance for NH_2, CH_3 and ring C–H stretching vibrations. The investigated molecule has only one NH_2 group and hence one symmetric and one asymmetric N–H stretching vibrations in NH_2 group are expected. The asymmetric stretching for the NH_2, CH_2 and CH_3 has magnitude higher than the symmetric stretching [29]. The asymmetric NH_2 stretching vibration appears from 3420 to 3500 cm^{-1} and the symmetric NH_2 stretching is observed in the range 3340–3420 cm^{-1} [30]. With reference to these, in this study, the vibrational frequencies described by modes 3 and 4 assigned to the N–H asymmetric and symmetric stretching modes, respectively. As expected these two modes are pure stretching modes as it is evident from TED column, they are almost contributing 100%. The corresponding symmetric mode occurs in the experiment at 3393 cm^{-1} and asymmetric mode at 3507 cm^{-1}. The vibrational NH_2 scissoring deformation appears in the 1638–1575 cm^{-1} region with strong to very strong IR intensity [29]. The recorded strong band at 1591 cm^{-1} is identified with NH_2 scissoring which also contributes with C–C stretching mode. This value deviates negatively by ca. 15 cm^{-1} from expected characteristic value. The wagging (torsion) and rocking fundamentals are assigned to the calculated bands at 227 cm^{-1} and 1036 cm^{-1} for the investigated molecule. The NH_2 twisting vibration calculated at 599 cm^{-1} is missing in FT-IR spectrum. The C–NH_2 stretching mode was obtained at 1233 cm^{-1} and 1453 cm^{-1} in the experimental FT-IR spectrum of 2-ATA coupled with the ring modes.

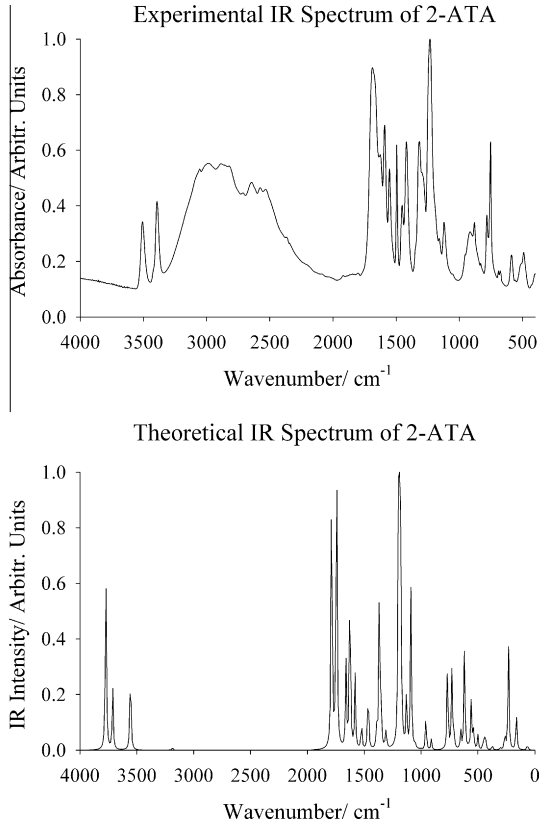

Fig. 2. The recorded and simulated infrared spectrum of 2-ATA.

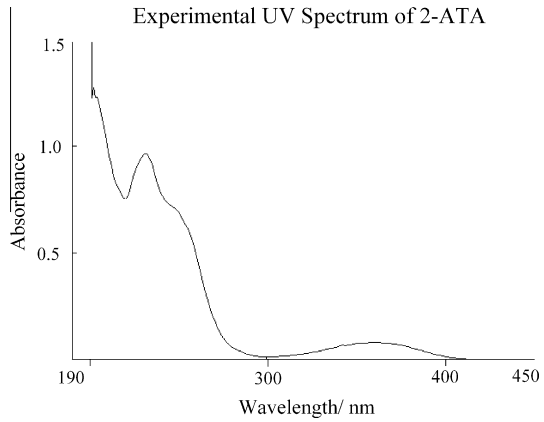

Fig. 3. The experimental UV spectrum of 2-ATA.

For all the aromatic compounds the carbon–hydrogen stretching vibrations are observed in the region 3000–3100 cm^{-1} [27,28,31]. In the present study, the three adjacent hydrogen atoms around the ring give rise three C–H stretching modes (5–7). In our calculations, C–H stretching vibrations are predicted in the range 3052–3090 cm^{-1}. They are very pure modes since their TED contribution are 100%. However, just one band was recorded in this region which corresponds to 3055 cm^{-1} and show excellent agreement with predicted value. The C–H in-plane bending frequencies appear in the range of 1000–1300 cm^{-1} and C–H out-of-plane bending vibration in the range 750–1000 cm^{-1} in the aromatic compounds. The vibration modes of 13, 18 and 22 are assigned the in-plane C–H bending even though found to be contaminated by other stretching vibrations. The calculated three vibrations (modes 26, 28 and 29 in Table 2) are assigned to out-of-plane C–H bending. In general the aromatic C–H vibrations (stretching, in-plane and out-of-plane bending) calculated theoretically are in good agreement with experimentally accepted values. The change in the frequencies of these deformations from the values in benzene is almost determined exclusively by the relative position of the substituents and is almost independent of their nature [32].

The O–H stretching is characterized by a very broad band appearing near about 3400 cm^{-1} [27,29]. On the other hand, the hydrogen bonding in the condensed phase with the other acid molecules makes vibrational spectra more complicated. Therefore, we could not observe the strong and sharp bands of the O–H vibration in the FT-IR spectrum. In the Raman spectrum of solid terephthalic acid, the Raman shift over 3000 cm^{-1} could not be observed and the calculated value at 3653 cm^{-1} is assigned to O–H stretching modes of the carboxylic groups [6]. When the OH in carboxylic acid do not form intramolecular bond the stretching mode is to be expected at 3520 cm^{-1} [3,27]. In this study the O–H stretching modes were calculated and assigned at 3616 and 3611 cm^{-1} for first (CA1) and second (CA2) carboxylic acid groups, respectively. For the studied molecule, the O–H in-plane and out-of-plane bending vibrations are computed at 1179, 1166 cm^{-1} and 549, 608 for CA1 and CA2, respectively.

The most characteristic feature of carboxylic group is a single band observed usually in the range 1690–1655 cm^{-1} region [33,34] and this band is due to the C=O stretching vibration. The band appearing at 1686 cm^{-1} as a very strong band in FT-IR is assigned to C=O stretching vibration. This is in agreement with our earlier report [35,36]. The theoretically computed values of

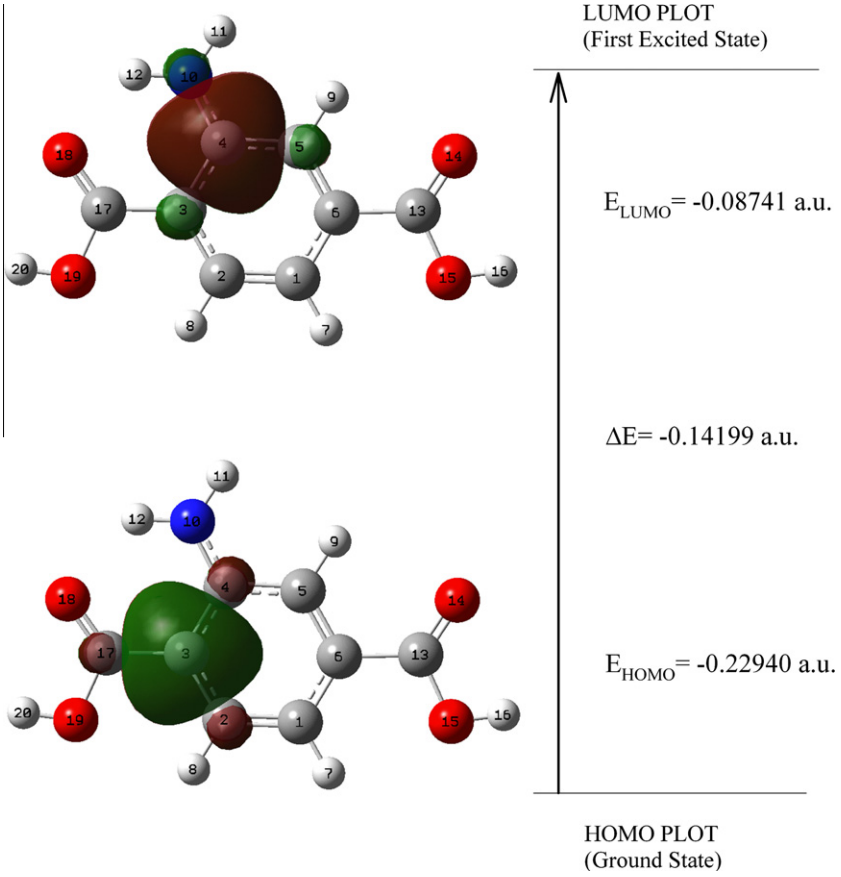

Fig. 4. The frontier molecular orbitals (HOMO and LUMO) for 2-ATA by using B3LYP.

Table 3
Calculated wavelengths λ (nm), excitation energies (eV), oscillator strengths (f), absolute energies (Hartree), frontier orbital energies (a.u.) and dipole moment (Debye) in gas phase and ethanol solution.

Gas				Ethanol	
λ (nm)	E (eV)	f	λ (nm)	E (eV)	f
365.41	3.3930	0.0869	378.70	3.2739	0.1096
270.18	4.5889	0.0000	265.08	4.6772	0.0000
260.45	4.7604	0.0000	257.95	4.8065	0.0000
	E_{HOMO}	E_{LUMO}	ΔE	μ (D)	
Gas	−0.22940	−0.08741	−0.14199	0.9016	
Ethanol	−0.22420	−0.08517	−0.13903	1.1796	

1670 and 1712 cm^{-1} (mode Nos. 8 and 9) show agreement with the experimental result. The C=O double bond stretching are assigned as pure modes.

Empirical assignments of vibrational modes for peaks in the fingerprint region are difficult. In the wavenumber region of 600–1660 cm^{-1}, the spectrum observed in the experiments closely resembles the calculated spectrum, except for differences in details. The ring carbon–carbon stretching vibrations occur in the region 1400–1650 cm^{-1} in benzene derivates. Varsanyi [31] observed five bands, 1625–1590, 1590–1575, 1540–1470, 1465–1430 and 1380–1280 cm^{-1}, in this region. Here, the skeletal vibrations (ring CC) were assigned in the region 915–1591 cm^{-1} and 941–1626 cm^{-1} experimental and theoretically. The ring breathing mode at 745 cm^{-1} coincides satisfactorily with recorded value of 753 cm^{-1} in FT-IR spectrum. The theoretically calculated CCC out-of-plane bending modes have been found to be consistent with the recorded spectral values. In the Infrared spectrum of 2-ATA, most of the bands in the region 2500–2900 cm^{-1} may also be due to the non-fundamental bands of the benzene ring. These vibrational bands are very sharp, broad and less intense. All these bands were assigned in terms of various fundamentals, overtone and combination vibrations. The details are described in Table 2. The remainders of the observed and calculated wavenumbers and assignments are also accounted in Table 2.

4.3. Electronic properties and UV spectra

The UV spectrum of 2-ATA is shown in Fig. 3, was measured in ethanol solution. It is observed that the absorption bands centered at 231 and 360 nm. In order to understand electronic transitions of steady compound, time-dependent DFT (TD-DFT) calculations on electronic absorption spectrum in vacuum and solvent were performed. Both the highest occupied molecular orbital (HOMO) and the lowest unoccupied molecular orbital (LUMO) are the main orbital taking part in chemical reaction. The HOMO energy characterizes the ability of electron giving; LUMO characterizes the ability of electron accepting [37]. The energy gap between the highest occupied and the lowest unoccupied molecular orbitals characterize the molecular chemical stability and it is a critical parameter in determining molecular electrical transport properties because it is a measure of electron conductivity. The energy gaps are largely responsible for the chemical and spectroscopic properties of the molecules [38]. This is also used by the frontier electron density for predicting the most reactive position in π-electron systems and also explains several types of reaction in conjugated system [39]. The features of the HOMO and LUMO can be seen in Fig. 4 for gas phase. The calculated frontier orbital energies, absorption

wavelengths (λ), oscillator strengths (f), excitation energies (E) and dipole moments are given in Table 3.

5. Conclusion

In this work, we have performed the experimental and theoretical vibrational and electronic transition analysis of 2-ATA. In order to identify its conformational structure the quantum chemical calculations were used. Based on the calculated energy differences, the C1 conformer is found to be the most stable conformer. SQM force fields have also been used to calculate potential energy distributions in order to make conspicuous vibrational assignments. A comparison of the result of experimental and theoretical study gave us a full description of the geometry, vibrational and electronic properties of studied compound.

Acknowledgements

We thank Dr. Levent Özcan for UV spectrum measurement, Afyon Kocatepe University, Department of Chemistry, Afyonkarahisar, Turkey.

Appendix A. Supplementary material

Supplementary data associated with this article can be found, in the online version, at doi:10.1016/j.molstruc.2010.07.033.

References

[1] M.J. Astle, Chemistry of Petrochemicals, Reinhold, New York, 1956. p. 174.
[2] M. Bailey, C.J. Brown, Acta Cryst. 22 (1967) 387–391.
[3] S.C. Tellez, A. Claudio, E. Hollauer, M.A. Mondragon, V.M. Castano, Spectrochim. Acta A 57 (2001) 993–1007.
[4] P.G. Jones, J. Ossowski, P. Kus, I. Dix, Z. Naturforsch. 64B (2009) 865–870.
[5] J.C. Barreto, G.S. Smith, N.H.P. Strobel, P.A. McQuillin, T.A. Miller, Life Sci. 56 (1994) 89–96.
[6] S.C. Tellez, A. Claudio, E. Hollauer, T. Giannerini, M.I. Pais da Silva, M.A. Mondragon, J.R. Rodriguez, V.M. Castano, Spectrochim. Acta A 60 (2004) 2171–2180.
[7] C.B. Liu, C.Y. Sun, L.P. Jin, S.Z. Lu, New J. Chem. 28 (2004) 1019–1026.
[8] Z. Rzaczynska, M. Wozniak, W. Wolodkiewicz, A. Ostasz, S. Pikus, J. Therm. Anal. Cal. 91 (2008) 951–956.
[9] J. Arias-Pardilla, H.J. Salavagione, C. Barbero, E. Morallon, J.L. Vazquez, Eur. Polym. J. 42 (2006) 1521–1532.
[10] C.A. Southern, D.H. Levy, G.M. Florio, A. Longarte, T.S. Zwier, J. Phys. Chem. A 107 (2003) 4032–4040.
[11] J. Brüning, J.W. Bats, M.U. Schmidt, Acta Cryst. E65 (2009) o2468–o2469.
[12] C. Lee, W. Yang, R.G. Parr, Phys. Rev. B 37 (1988) 785.
[13] A.D. Becke, J. Chem. Phys. 98 (1993) 5648.
[14] J.B. Foresman, E. Frisch, Exploring Chemistry with Electronic Structure Methods: A Guide to Using Gaussian, Gaussian, Pittsburgh, PA, 1993.
[15] A.P. Scott, L. Radom, J. Phys. Chem. 100 (1996) 16503.
[16] M. Karabacak, M. Kurt, M. Cinar, A. Coruh, Mol. Phys. 107 (2009) 253–264.
[17] N. Sundaraganesan, S. Ilakiamani, H. Saleem, P.M. Wojciechowski, D. Michalska, Spectrochim. Acta A 61 (2005) 2995–3001.
[18] G. Rauhut, P. Pulay, J. Phys. Chem. 99 (1995) 3093.
[19] J. Baker, A.A. Jarzecki, P. Pulay, J. Phys. Chem. A 102 (1998) 1412.
[20] M.J. Frisch et al., Gaussian 03, Revision B. 4, Gaussian Inc., Pittsburgh, PA, 2003.
[21] J.C.D. Brand, D.R. Williams, T.J. Cook, J. Mol. Spectrosc. 20 (1966) 359–380.
[22] D.G. Lister, J.K. Tyler, J.H. Hog, N.W. Larsen, J. Mol. Struct. 23 (1974) 253–264.
[23] W.E. Sinclair, D.W. Pratt, J. Chem. Phys. 105 (1996) 7942–7956.
[24] O. Bludsky, J. Sponer, J. Leszczynski, V. Spirko, P. Hobza, J. Chem. Phys. 105 (1996) 11042–11050.
[25] J.C. Jiang, C.E. Lin, J. Mol. Struct. (THEOCHEM) 392 (1997) 181–191.
[26] I. Lopez-Tocon, Chem. Phys. Lett. 327 (2000) 45–53.
[27] M. Silverstein, G.C. Basseler, C. Morill, Spectrometric Identification of Organic Compounds, Wiley, New York, 1981.
[28] V. Krishnakumar, R. Ramasamy, Spectrochim. Acta Part A 62 (2005) 570.
[29] D. Lin–Vien, N.B. Colthup, W.G. Fateley, J.G. Grasselli, The Handbook of Infrared and Raman Characteristic Frequencies of Organic Molecules, Academic Press, Boston, MA, 1991.
[30] L.J. Bellamy, The Infrared Spectra of Complex Molecules, vol. 2, Chapman and Hall, London, 1980.
[31] G. Varsanyi, Assignments of Vibrational Spectra of 700 Benzene Derivatives, Wiley, New York, 1974.
[32] N. Sundaraganesan, H. Saleem, S. Mohan, Spectrochim. Acta A 59 (2003) 2511–2517.
[33] C.B. Smith, Infrared Spectral Interpretation, CRC Press, New York, 1999.
[34] G. Socrates, Infrared and Raman Characteristic Group Frequencies, John Wiley, New York, 2001.
[35] M. Karabacak, M. Cinar, M. Kurt, J. Mol. Struct. 885 (2008) 28–35.
[36] M. Karabacak, M. Cinar, S. Ermec, M. Kurt, J. Raman Spectrosc. 41 (2010) 98–105.
[37] K. Fukui, Science 218 (1982) 747.
[38] P.W. Atkins, Physical Chemistry, Oxford University Press, Oxford, 2001.
[39] K. Fukui, T. Yonezawa, H. Shingu, J. Chem. Phys. 20 (1952) 722.